Automated quality assurance of deep learning contours in head-and-neck radiotherapy
Mody, P.P.

2

Large-scale dose evaluation of deep learning organ contours in head-and-neck radiotherapy by leveraging existing plans

Abstract

Background and Purpose: Retrospective dose evaluation for organ-at-risk auto-contours has previously used small cohorts due to additional manual effort required for treatment planning on auto-contours. We aimed to do this at large scale, by a) proposing and assessing an automated plan optimization workflow that used existing clinical plan parameters and b) using it for head-and-neck auto-contour dose evaluation.

Materials and Methods: Our automated workflow emulated our clinic's treatment planning protocol and reused existing clinical plan optimization parameters. This workflow recreated the original clinical plan (P_{OG}) with manual contours (P_{MC}) and evaluated the dose effect ($P_{OG} - P_{MC}$) on 70 photon and 30 proton plans of head-and-neck patients. As a use-case, the same workflow (and parameters) created a plan using auto-contours (P_{AC}) of eight head-and-neck organs-at-risk from a commercial tool and evaluated their dose effect ($P_{MC} - P_{AC}$).

Results: For plan recreation ($P_{OG} - P_{MC}$), our workflow had a median impact of 1.0% and 1.5% across dose metrics of auto-contours, for photon and proton respectively. Computer time of automated planning was 25% (photon) and 42% (proton) of manual planning time. For auto-contour evaluation ($P_{MC} - P_{AC}$), we noticed an impact of 2.0% and 2.6% for photon and proton radiotherapy. All evaluations had a median ΔNTCP (Normal Tissue Complication Probability) less than 0.3%.

Conclusions: The plan replication capability of our automated program provides a blueprint for other clinics to perform auto-contour dose evaluation with large patient cohorts. Finally, despite geometric differences, auto-contours had a minimal median dose impact, hence inspiring confidence in their utility and facilitating their clinical adoption.

2.1 Introduction

Manual contouring of organs-at-risk (OAR) in radiotherapy is a time and resource-demanding task [5, 93, 94], especially in head-and-neck cancer due to a large OAR count [95]. Moreover, it is plagued by inter- and intra-annotator variability [10, 11, 96, 97] and hence there is a need for automation. In the last few years, availability of deep learning-based commercial tools have reduced the barriers for clinics to implement auto-contouring technology in daily practice. However, these tools may produce erroneous contours due to poor contrast, organ deformations, surgical removal of an organ or when tested on different patient cohorts [98]. Such cases may potentially lead to commercial providers providing updates to the underlying deep learning models. Thus, as deep learning auto-contouring tools are increasingly adopted in clinics, with the potential for future updates to models, there is a growing need to benchmark them, preferably at large-scale and in an automated manner.

As deep learning-based auto-contouring methods for head-and-neck OARs have been shown to offer satisfactory geometric performance [10, 99], the next step is to evaluate their dose impact [100]. However, we observed that dose-based studies on auto-contours tend to use either smaller (≤ 20) [41, 45, 46, 48, 49, 101, 102] or medium-sized (≤ 40) [50], rather than larger [47] datasets. Studies using larger datasets simply superimpose the automated contours on the clinical dose [47] which does not fully replicate the treatment planning process. Conversely, studies using smaller or medium-sized test datasets either made manual plans [41, 48–50], used knowledge-based planning [46], a template approach [45] or a priori multi-criteria optimization (MCO) [101, 102]. Since smaller datasets may be affected by sampling bias, there is a need to perform dose analysis with a larger patient cohort. However, a manual approach to plan optimization is simply not scalable. Moreover, existing automated approaches [45, 46, 101], if not already clinically implemented, require additional skills and resources. Therefore, there is a need for an automated approach to treatment planning that can be done at a large scale and also leverages existing clinical knowledge and work.

Thus, our contribution was to propose and assess a plan optimization method for retrospective studies that is scalable due to its automated nature and easily implementable due to the use of existing clinical resources (i.e., knowledge, tools and optimization parameters). We then used this approach in a use case to quantify auto-contour-induced dose effects for head-and-neck photon and proton radiotherapy.

2.2 Materials and methods

2.2.1 Data acquisition

Our dataset consists of 100 head-and-neck cancer patients, of which 70 had clinical plans made for photon therapy, while 30 had proton plans, at Leiden University Medical Center
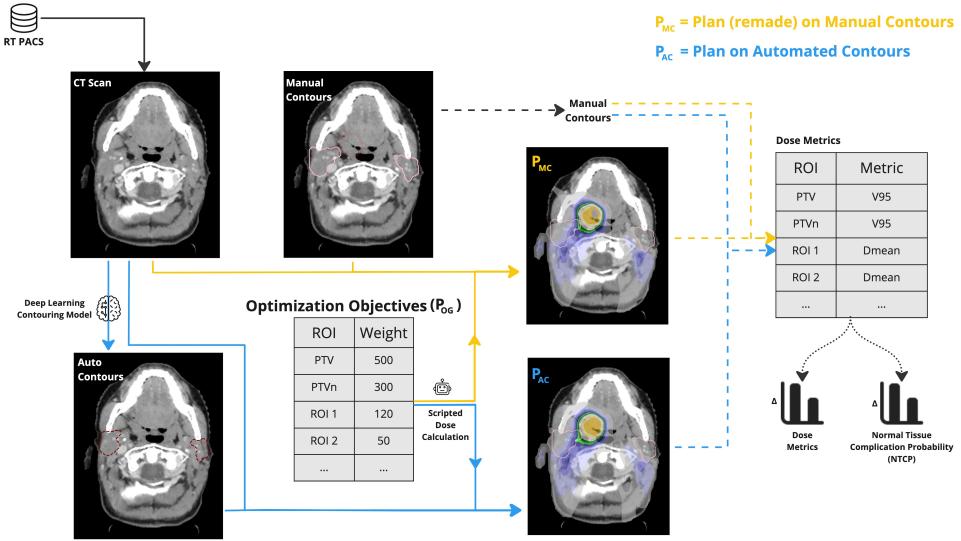
Figure 2.1: Workflow for automated plan optimization and use-case of evaluating the effect of automated contours on dose. By reusing original plan (P_{OG}) parameters, we made a plan for both the manual contours (P_{MC}) and automated contours(P_{AC}), shown with yellow and blue colors respectively. Dashed lines indicate the evaluation workflow where both doses were evaluated on the manual contours. Pink, maroon and orange contours are used to represent the manual, automated and PTV (DL1) contours respectively. Finally, we used manual contours to compute dose metrics and normal tissue complication probability (NTCP) [103] models and compare all plans.

(Leiden, The Netherlands) from 2021 to 2023. Patients were treated for either oropharyngeal (71) or hypopharyngeal (29) cancers with cancer stages T1-4, N0-3 and M0. 92 patients were treated with curative intent, i.e., 7000cGy to the primary tumor, while others were prescribed 6600cGy due to their post-operative nature. Details about CT scans used in planning are written in Section 2.6.1. The study was approved by the Medical Ethics Committee of Leiden, The Hague, Delft (G21.142, October 15, 2021). Patient consent was waived due to the retrospective nature of the study.

2.2.2 Automated Contours

For automated contouring, a commercial deep learning model from RayStation-10B (Ray-Search Labs, Sweden) - "RSL Head and Neck CT" (v1.1.3) was used. A subset of the OARs which were used clinically for treatment planning were auto-contoured – Spinal Cord, Brainstem, Parotid (L/R), Submandibular (L/R), Oral Cavity, Esophagus, Mandible and Larynx (Supraglottic). See Section 2.6.2 for additional details.

2.2.3 Treatment Planning Protocol

We used volumetric modulated arc therapy (VMAT) to generate a photon plan using a 6MV dual arc beam. The elective and boost Planning Target Volumes (PTV), henceforth referred as DL1/DL2 (dose level 1/2) were prescribed 5425cGy/7000cGy in 35 fractions. For post-operative patients, our clinic prescribed 5280cGy/6600cGy in 33 fractions instead. Planning was done such that at least 98% of DL1 and DL2 volumes received 95% of the prescribed dose ($V_{95\%}$) and also by keeping $D_{0.03cc}$ for DL2 below 107% of the prescribed dose.

Proton plans consisted of six beam intensity modulated proton therapy (IMPT). Planning was done such that $V_{95\%} \geq 98\%$ for DL1/DL2 and $D_{2\%} \leq 107\%$ for DL2 of the Clinical Target Volume (CTV) in a 21-scenario robust optimization with 3mm setup and 3% proton range uncertainty. For robust evaluation of CTV DL1/DL2 we instead use 28-scenarios and test the voxel-wise minimum (vw-min) plan such that its $V_{94\%} \geq 98\%$ [104] and voxel-wise maximum (vw-max) of $D_{2\%} \leq 107\%$.

2.2.4 Automated Treatment Planning

To make our automated program, a four-step script [105–107] was created which uses manually defined beam settings and objective weights from the clinical plan (more details in Section 2.6.3). This approach is also referred as robot process automation (RPA) [108], a process wherein a program emulates a human.

In summary, for step 1, we began with an objective template i.e., a class solution with a standard set of weights that focuses on targets and the body contour. Step 2 then added dose-fall-off (DFO) objectives for organs which is the distance over which a specified high dose falls to a specified low dose. In step 3, we introduced equivalent uniform dose (EUD) objectives [109] on the OARs. Manual planning for the EUD objective involves iteratively fine-tuning its parameters. Since only the parameters of the last iteration were available to us, we instead followed a single-step optimization for this objective. Finally, in step 4, we used patient-specific control structure contours to reduce OAR dose or sculpt the dose to the targets. In the last step, we also updated any other weights the treatment planner might have changed compared to the objective template. Note, these final weight updates were asynchronous to manual planning, since we did not know when these weights were updated in the aforementioned process. Note that each of the above steps underwent four optimization cycles.

Using our automated program, we made two plans – 1) a plan optimized on manual contours (P_{MC}) and 2) a plan optimized on automated contours (P_{AC}) as shown in Figure 5.1. For the targets, elective lymph nodes, and OARs not available in the auto-contouring model we used manual contours which were used clinically for the original plan (P_{OG}). The plans were made using the Python 3.6 scripting interface of the Treatment Planning System (TPS) of RayStation. The scripts for this work are available at
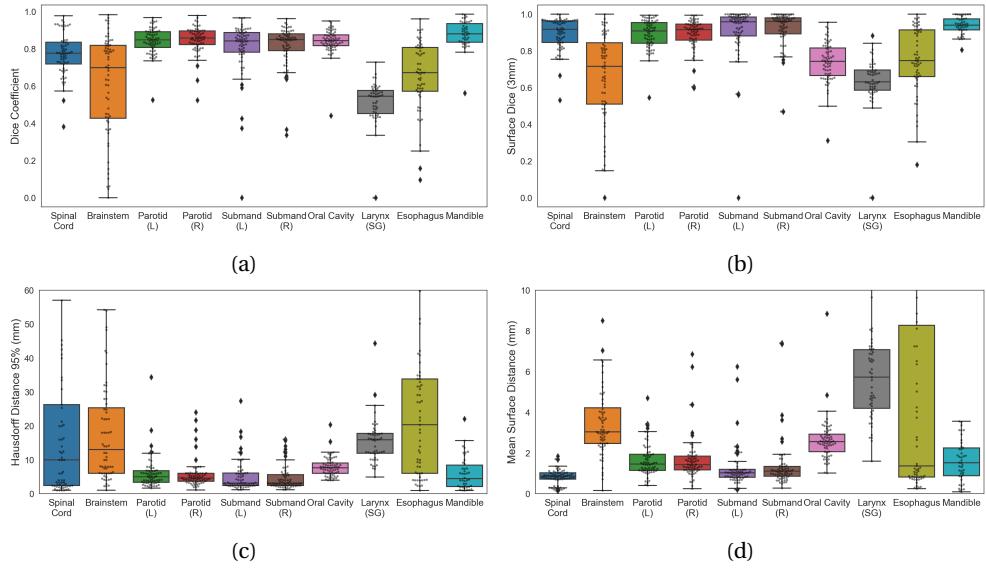
Figure 2.2: Box plots showing geometric (a) and surface metrics (b,c,d) for all our patients. The scatter points indicate the metric values for each patient.

https://github.com/prerakmody/dose-eval-via-existing-plan-parameters.

2.2.5 Geometric Evaluation

We used volumetric and surface distance metrics like Dice Coefficient, Hausdorff Distance 95% (HD95) and Mean Surface Distance (MSD) to evaluate our contours. Moreover, we also evaluated Surface DICE (SDC) with a margin of 3mm to gain insight into contour editing time requirements [110].

2.2.6 Dose and NTCP Evaluation

Given that our plans – P_{OG}, P_{MC} and P_{AC} have differences in the way they were created, we need to compare them. Metrics relevant to OARs were calculated and plans were compared in the following manner:

$$\Delta D_x = D_{x,p1} - D_{x,p2}. \tag{2.1}$$

Here, x refers to the OAR for which we calculated a dose metric D and then compared it between any pair of plans $p1$ and $p2$. Here, D can refer to $D_{0.03cc}$ (Spinal Cord, Brainstem), D_{mean} (Parotid, Submandibular, Oral Cavity, Larynx (Supraglottic), Esophagus) or $D_{2\%}$ (Mandible).

For normal tissue complication (NTCP) probability [103] evaluation, we used a similar approach:

$$\Delta \text{NTCP}_d = \text{NTCP}_{d,p1} - \text{NTCP}_{d,p2}, \tag{2.2}$$

14

(a) Organs at Risk

(b) Targets

(c) NTCP
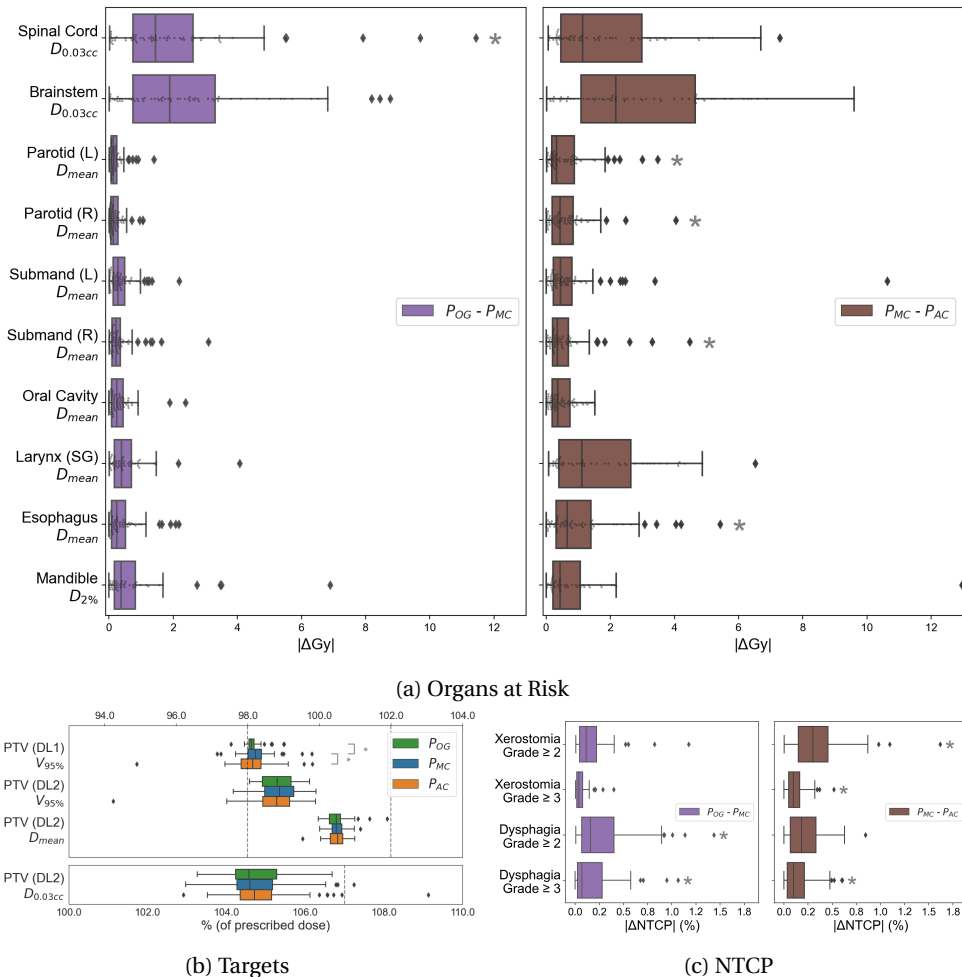
Figure 2.3: Dose metrics for the original (i.e., clinical) photon plans (P_{OG}) as well as plans (re)made on manual (P_{MC}) and automated (P_{AC}) contours using an automated program. $P_{OG}-P_{MC}$ shows the dose effect of the proposed planning process, while $P_{MC}-P_{AC}$ shows the effect of using auto-contours. Here * represents a p-value ≤ 0.05. In a) we see the difference in the dose metric of each OAR when comparing across plans. The plots in b) show us the metrics for the targets, while c) shows us the difference in NTCP values.

where d refers to either Xerostomia or Dysphagia with a grade ≥ 2 or ≥ 3.

For the above ΔD_x (dose) and $\Delta \mathrm{NTCP}_d$ values, we performed a Wilcoxon signed-rank test (p ≤ 0.05 is considered a significant difference) to evaluate if the differences between plans are significant.

2.3 Results

2.3.1 Geometric evaluation

Figure 2.2 shows five organs (Spinal Cord, Parotids, Submandibulars, Oral Cavity, Mandible) had a median DICE ≥ 0.78 (with additional summary measures tabulated in Section 2.6.2). In Figure 2.2b we observed that in general the surface DICE values for the OARs are higher than their DICE values, except for the oral cavity. Figure 2.2c and Figure 2.2d shows that HD95 and MSD had trends similar to DICE in Figure 2.2a. OARs with a median DICE ≥ 0.8 had their median HD95 less than 7.7mm and their median MSD less than 2.6mm. The spinal cord had DICE values that are better than brainstem, but its HD95 range was as long as brainstem.

2.3.2 Dose evaluation

The median absolute value of P_{OG} (original plan) - P_{MC} (automated plan using manual contours) was 0.27Gy (1.0%), 1.66Gy (4.6%) and 0.21Gy (0.7%) for all, central nervous system (CNS), i.e., Brainstem and Spinal Cord and non-CNS organs, respectively. The same for P_{MC} - P_{AC} (automated plan using auto-contours) was 0.58Gy (2.0%), 1.86Gy (5.4%) and 0.46Gy (1.6%), with metrics of individual organs in Figure 2.3a listed in Section 2.6.4. Figure 2.3b shows dose metrics for targets where, for P_{MC} and P_{AC}, we achieved PTV (DL1) (V_{95}) ≥ 98.0% for 76% and 60% of plans. However, 96% and 93% of P_{MC} and P_{AC} plans achieved PTV (DL1) (V_{95}) ≥ 97.5%. For this metric, a statistically significant difference was observed between P_{OG} and P_{MC} as well as P_{MC} and P_{AC}. Finally, Figure 2.3c shows |ΔNTCP| results, where the maximum median across all toxicities was 0.3% (individual toxicity metrics in Section 2.6.5).

For proton, $|P_{OG} - P_{MC}|$ had a median value of 0.33Gy (1.5%), 1.13Gy (11.5%) and 0.22Gy (0.8%) for all, CNS and non-CNS organs, respectively. The same for $P_{MC} - P_{AC}$ was 0.48Gy (2.6%), 0.75Gy (6.9%) and 0.38Gy (1.8%). Figure 2.4b shows proton targets wherein 58% and 62% of P_{MC} and P_{AC} plans achieved PTV (DL1) (vw-min) (V_{94}) ≥ 98.0%, while 82% and 80% achieved PTV (DL1) (vw-min) (V_{94}) ≥ 97.5%. Similar to photon, a statistically significant difference was observed between P_{OG} and P_{MC} as well as P_{MC} and P_{AC}. For |ΔNTCP| (Figure 2.4c), the maximum median across all toxicities was 0.2%.

A weak Spearman correlation coefficient between DICE and dose differences ($|P_{MC} - P_{AC}|$) was observed for CNS organs ($|\rho_s| \leq 0.11$), across both photon and proton (Figure 2.5). Conversely, the Parotids, Submandibulars and Oral Cavity had relatively higher values ($-0.43 \leq \rho_s \leq -0.17$). The remaining organs did not have similar correlations across both radiotherapy treatments.

Finally, our automated plan optimization took 45 minutes and 2.5 hours of computer time, compared to 3 and 6 hours of manual time (on average, as estimated by our clinic's planners), for photon and proton, respectively.

(a) Organs at Risk

(b) Targets

(c) NTCP
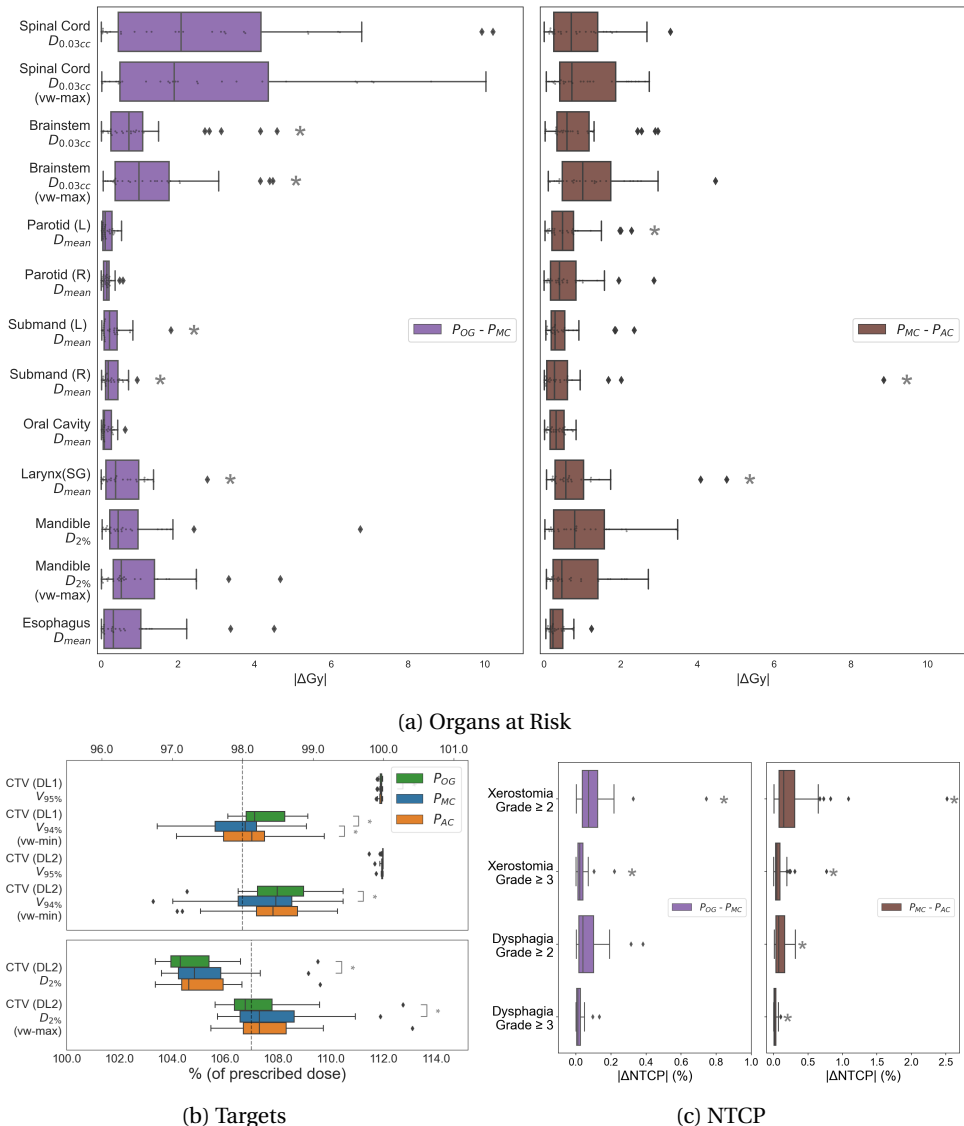
Figure 2.4: Dose metrics for the original proton plans (P_{OG}) as well as plans (re)made on manual (P_{MC}) and automated (P_{AC}) contours using an automated program. $P_{OG} - P_{MC}$ shows the dose effect of the proposed planning process, while $P_{MC} - P_{AC}$ shows the effect of using auto-contours. Here * represents a p-value ≤ 0.05. In a) we see the difference in the dose metric of each OAR when comparing across plans. The plots in b) show us the metrics for the targets, while c) shows us the difference in NTCP values.
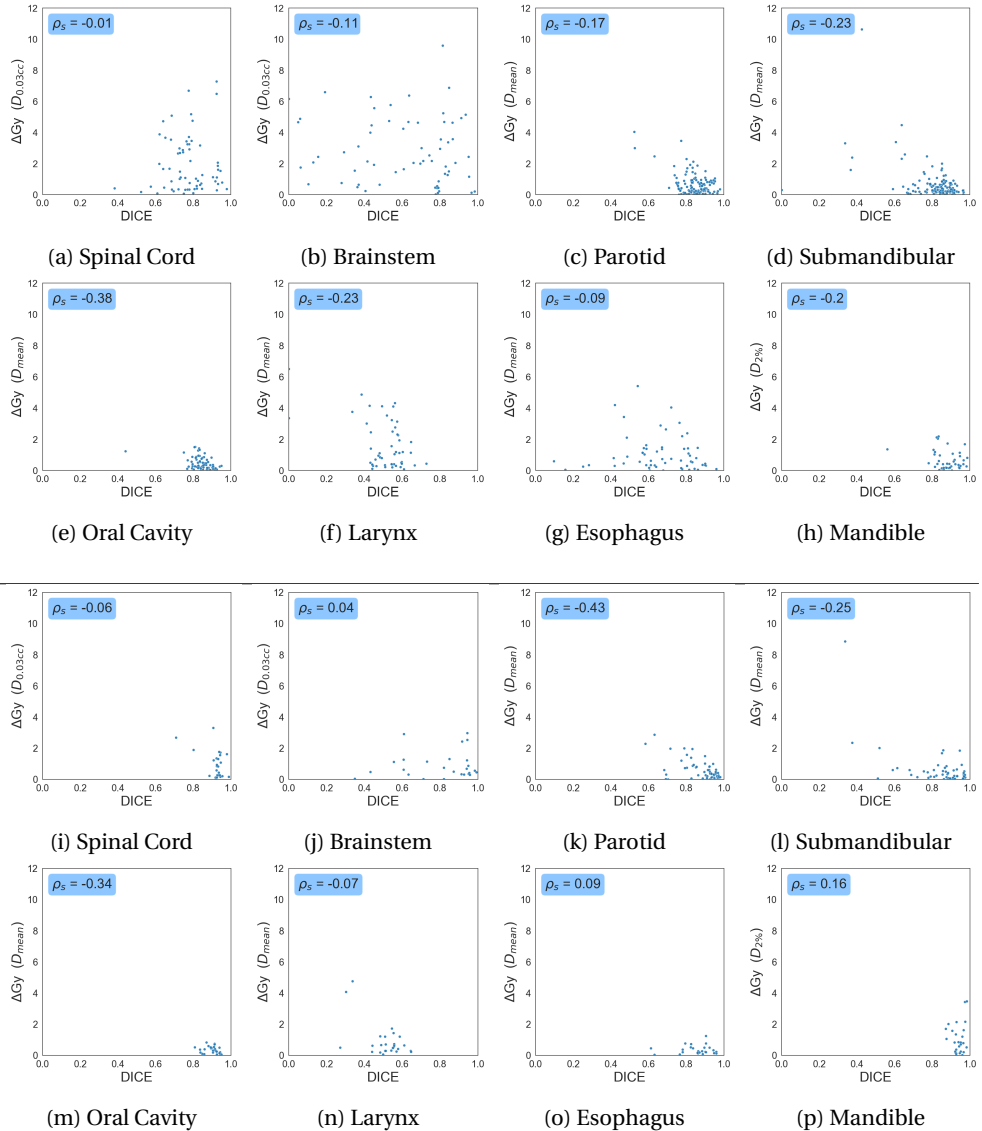
Figure 2.5: Scatter plots for eight organs-at-risk from the auto-contouring module. Here we plot the DICE (x-axis) against each organs absolute dose metric differences, i.e., $|P_{MC} - P_{AC}|$ (y-axis) for photon (a-h) and proton (i-p) radiotherapy.

2.4 Discussion

This work aimed at proposing and assessing an automated plan optimization workflow for retrospective studies that can be easily implemented by clinics due to its use of existing clinical resources. Unlike previous works [41, 45, 46, 48, 49, 101, 102], we performed this

18

at large-scale and for both photon and proton radiotherapy. To replicate our approach, a clinic can simply use the scripting interface of their treatment planning system (TPS) and convert their planning process into a step-by-step approach. This requires minimal additional expertise (i.e., Python coding), for which many TPS solutions provide documentation. For head-and-neck radiotherapy, automated plans on manual contours (P_{MC}) showed a negligible difference (i.e., median impact of 1.0% and 1.5% across organs), when compared to the original clinical plan (P_{OG}) [111, 112]. Thus, the proposed evaluation process could serve as a springboard for clinics to validate an auto-contouring model, at large-scale, by simply reusing their existing plans. When using this program for the use case of head-and-neck auto-contour evaluation, the plan using auto-contours (P_{AC}) had a low dose impact when compared to the plan using using manual organ contours, for both photon (2.0%) and proton (2.6%) planning. Additionally, minuscule differences in NTCP values indicated that minor plan differences did not lead to large differences in long-term radiation-induced toxicity. This could potentially promote confidence in the community [113] to adopt auto-contouring to speed up clinical workflows.

For five out of eight OARs (i.e., Spinal Cord, Parotid, Submandibular, Oral Cavity and Mandible), the average DICE scores may be considered on par with previous work (≈ 0.8) [10, 45, 99] (see Section 2.6.2). A visual inspection of the remaining auto-contours, i.e., Larynx (SG), Brainstem (and by extension the Spinal Cord) (Figure 2.6, Section 2.6.6) indicated that they had contouring protocols that differed from our clinic. Moreover, the auto-contouring model was trained on a different patient cohort, leading to additional contour differences with our clinical dataset. Finally, we chose to not perform any additional refinement on manual contours, since they were also used for making clinical plans (P_{OG}) delivered to patients. For e.g. in the first row of Figure 2.6, we see that only the caudal section of the Brainstem was annotated. Treatment planners find optimizing this section sufficient due to its potential for high dose from tumor proximity. The aforementioned reasons are why we noticed reduced measures for Larynx (SG), Brainstem and Spinal Cord in Figure 2.2.

A critique of using unmodified manual contours may be that a lack of "gold-standard" contours will not give accurate geometric measures. Since our primary goal however was dose evaluation using existing clinical resources (i.e., unmodified manual contours), we proceed without any refinement. Also, in an auto-contouring dose evaluation scenario, it is already sufficient to know that plans made on auto-contours are equivalent to plans made on manual contours as seen in Figure 2.3b (photon) and Figure 2.4b (proton). Thus, our approach of using existing manual contours improves the ease-of-implementation of auto-contour dose evaluation studies and enables evaluation at large-scale.

To evaluate the quality of our automated plans, we first assessed target dose metrics. We use PTV (DL1) ($V_{95\%}$) for photon and CTV (DL1) ($V_{94\%}$) (vw-min) for proton, since planners prioritize them due to their difficulty. Hence it serves as a good benchmark for

our automated plans. Results indicated that most of our plans ($\geq$ 93% for photon and $\geq$ 80% for proton) were of near-clinical quality (i.e., $\geq$ 97.5%). Those plans that did not strictly achieve clinical quality (i.e., $\geq$ 98%) on the aforementioned metrics, had reduced dose coverage in either the most cranial or caudal slices. In a retrospective study for dose-evaluation of auto-contours, such a minor error will have a minimal effect on the dose metrics of organs we are interested in.

Figure 2.4b shows that most proton plans, including P_{OG}, tended to have hotspots, i.e., $D_{2\%}(vw - max) \geq 107\%$, unlike most photon plans which did not, i.e., $D_{0.03cc} \leq 107\%$ (Figure 2.3b). In our dataset, these proton plans were made for performing a plan comparison between photon and proton (via NTCP), according to the model-based selection [114]. If during proton treatment planning, the NTCP differences already indicated either a) high organ sparing or b) not sufficiently better organ sparing than photons, planners did not further optimize this plan. However, given that dose hotspots are quite small, they did not affect dose metrics for the auto-contoured organs in our study. Finally, differences in plans were also caused because the same plan optimization process when run twice, may lead to similar, but not exactly the same solution due to randomness in initialization.

Figure 2.3 shows that of all the organs the Spinal Cord and Brainstem had wider box-plots for both $P_{OG} - P_{MC}$ and $P_{MC} - P_{AC}$. This is because the $\Delta D_{0.03cc}$ metric is inherently more sensitive to dose changes than ΔD_{mean}. This is seen in the first row of Figure 2.6 where similar DICE values for the Brainstem output vastly different dose differences. For proton (Figure 2.4), we saw a similar trend for $P_{OG} - P_{MC}$, but not for $P_{MC} - P_{AC}$. This indicated that proton planning is more susceptible to workflow differences than contour differences of Brainstem and Spinal Cord, for our cohort of oro- and hypopharyngeal cancers, which are at a distance from these organs.

Figure 2.3a, 2.3c (photon) and Figure 2.4a, 2.4c (proton) show statistically significant differences, but from a clinical standpoint, the minor differences in organ dose metrics and ΔNTCP values may be clinically irrelevant.

Moving on to the effect of DICE on dose metric of organs (Figure 2.5), one would expect that a decrease in DICE would lead to higher ΔcGy values for organs. This was true for the Parotids, Submandibulars (Figure 2.6) and Oral Cavity across both photons and protons ($-0.43 \leq \rho_s \leq -0.17$). The Brainstem and Spinal Cord showed poor correlation scores for both forms of radiotherapy, primarily due to the sensitive nature of the $D_{0.03cc}$ metric. The Esophagus also showed low correlation, since, in many cases, it is caudally far away from the tumor regions for the patients in our cohort. The Larynx showed a high correlation for photon, but not for proton, which could be an effect of sample size. Finally, the Mandible, an organ with high DICE, showed opposite trends in photon and proton. Overall, we noticed that there was a low correlation between DICE and dose metrics.

This work was inspired by prior research on treatment plan scripting [105, 106] to scale-up dose evaluation for auto-contours. However, some plans were still not of the

(a) Brainstem (DICE=0.13, $|\Delta D_{0.03cc}| = 6.0\%$)   (b) Brainstem (DICE=0.19, $|\Delta D_{0.03cc}| = 27.2\%$)

(c) Submand (R) (DICE=0.82, $|\Delta D_{mean}| = 1.7\%$)   (d) Submand (L) (DICE=0.42, $|\Delta D_{mean}| = 84.9\%$)

(e) Parotid (R) (DICE=0.85, $|\Delta D_{mean}| = 3.0\%$)   (f) Parotid (R) (DICE=0.63, $|\Delta D_{mean}| = 20.5\%$)

(g) Larynx (SG) (DICE=0.64, $|\Delta D_{mean}| = 0.5\%$)   (h) Larynx (SG) (DICE=0.55, $|\Delta D_{mean}| = 2.3\%$)
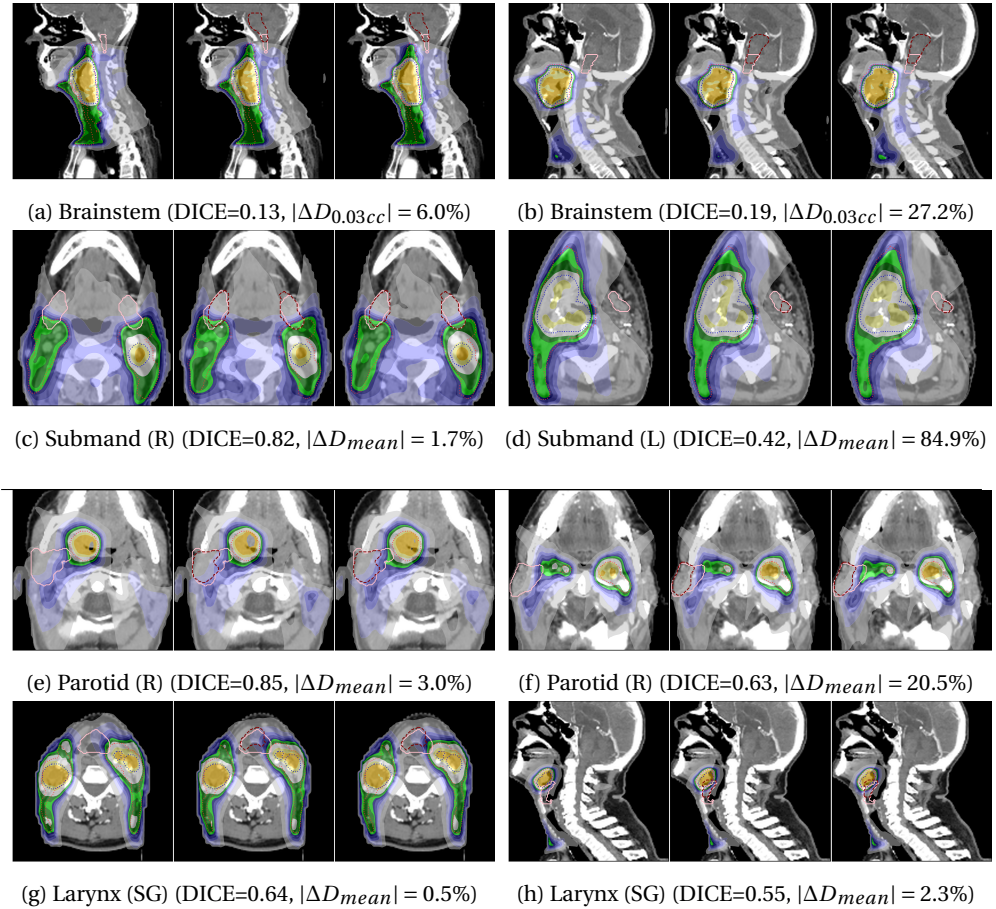
Figure 2.6: CT scans of photon (a-d) and proton (e-h) patients overlaid with a dose distribution as well as PTV (DL1) (orange), PTV (DL2) (blue), manual (pink) and automated (maroon) contours. Each example shows the P_{OG}, P_{MC} and P_{AC} plans from left to right. The dose metric in the sub-captions compares the absolute percentage difference of $P_{MC} - P_{AC}$.

highest possible quality since our four-step replication of the clinical process is a close, but imperfect emulation of a treatment planners approach. Non-iterative EUD optimization (step 3), lack of synchrony in weight updates between the manual and automated approach (step 4), and re-use of control structures from P_{OG} to P_{MC} and P_{AC} (step 4), led to small deviations from the original planning process. These limitations cause P_{MC} and P_{AC} dose metrics to be imprecise which could potentially impact our results. For future work we would like to more closely mimic the optimization steps as well as consider control structures specific to each plan, rather than simply copying them.

To conclude, we showed an automated approach to plan creation for retrospective

studies that was employed for the use-case of evaluating the dose impact of auto-contouring software, at scale. We hope our results showcasing low dose impact of auto-contours will inspire others to investigate and eventually use them in clinical settings.

2.5 Acknowledgement

2.6 Appendix

2.6.1 Data Acquisition

The CT scans of our dataset had a dimension of 512 x 512 pixels in the spatial plane with a pixel spacing in the range of [0.92-1.36] mm. Each CT slice was 2mm thick and each scan had between [128,199] slices. The scans were acquired from a Brilliance Big Bore (Philips Healthcare, Ohio, USA) with 120kV and 250mAs. Post acquisition, 64% of patients had Orthopedic Metal Artifact Reduction (O-MAR) processing done.

2.6.2 Automated Contours

The auto-contouring model of RayStation 10B (results in Table 2.1 and Table 2.2) first performed registration of the chosen CT scan using an atlas of CTs to narrow down CT size so it fits within the graphical processing unit (GPU) used for deep learning. Once registered, the mid-point of each OAR is detected and a 3D bounding box is cropped around that. This cropped area is then passed to a neural net trained for contouring that specific OAR. Each OAR-specific neural net is based on the UNet segmentation architecture whose output is a 3D probabilistic mask for that OAR. As a post-processing step, smoothing is performed on the surfaces of OARs. The model was trained using Tensorflow, an open-source deep neural net software package. During training, rotations, translations and elastic deformations were used to augment the training data. Details on patient cohort were not made public by the manufacturer.

RoI	DICE	SDC @ 3mm	HD95 (mm)	MSD (mm)
Spinal Cord ($D_{0.03cc}$)	0.78 [0.61,0.93]	0.92 [0.76,0.97]	10.0 [1.1,69.4]	0.9 [0.2,1.4]
Brainstem ($D_{0.03cc}$)	0.70 [0.07,0.95]	0.72 [0.18,0.95]	13.1 [2.5,49.0]	3.1 [1.1,8.3]
Parotid (L) (D_{mean})	0.85 [0.75,0.94]	0.91 [0.78,0.98]	5.0 [2.3,12.3]	1.5 [0.6,3.2]
Parotid (R) (D_{mean})	0.86 [0.74,0.94]	0.92 [0.75,0.98]	4.6 [2.2,15.7]	1.4 [0.6,4.2]
Submand (L) (D_{mean})	0.84 [0.59,0.93]	0.96 [0.74,1.00]	3.1 [1.7,16.3]	1.0 [0.5,5.3]
Submand (R) (D_{mean})	0.85 [0.68,0.92]	0.96 [0.75,1.00]	3.1 [1.7,16.3]	1.1 [0.6,3.5]
Oral Cavity (D_{mean})	0.84 [0.77,0.92]	0.74 [0.59,0.90]	7.7 [4.3,12.0]	2.6 [1.5,3.3]
Larynx (SG) (D_{mean})	0.54 [0.36,0.65]	0.63 [0.51,0.80]	15.9 [7.8,25.0]	5.7 [2.8,10.2]
Esophagus (D_{mean})	0.66 [0.28,0.90]	0.75 [0.41,0.97]	20.4 [2.5,63.9]	1.4 [0.3,18.8]
Mandible (D_{mean})	0.88 [0.81,0.97]	0.94 [0.87,1.00]	4.5 [1.1,14.0]	1.5 [0.2,3.4]

Table 2.1: Summary measures (median [5th percentile, 95th percentile]) for volumetric and surface metrics of auto-contours of RayStation 10B.

RoI	DICE	SDC @ 3mm	HD95 (mm)	MSD (mm)
Spinal Cord ($D_{0.03cc}$)	0.77 [0.74,0.80]	0.89 [0.87,0.91]	19.2 [13.6,24.7]	0.8 [0.7,0.9]
Brainstem ($D_{0.03cc}$)	0.61 [0.61,0.67]	0.66 [0.60,0.72]	18.0 [14.4,21.5]	3.8 [3.3,4.5]
Parotid (L) (D_{mean})	0.84 [0.84,0.86]	0.89 [0.87,0.91]	5.8 [4.8,6.8]	1.7 [1.5,1.8]
Parotid (R) (D_{mean})	0.85 [0.85,0.86]	0.89 [0.87,0.91]	5.8 [4.9,6.9]	1.7 [1.5,2.0]
Submand (L) (D_{mean})	0.80 [0.80,0.84]	0.90 [0.87,0.94]	6.2 [4.3,8.9]	2.3 [1.1,4.3]
Submand (R) (D_{mean})	0.82 [0.82,0.84]	0.92 [0.89,0.94]	4.8 [3.9,5.7]	1.4 [1.1,1.7]
Oral Cavity (D_{mean})	0.84 [0.82,0.86]	0.74 [0.71,0.76]	7.9 [7.2,8.6]	2.6 [2.4,2.9]
Larynx (SG) (D_{mean})	0.51 [0.47,0.54]	0.63 [0.58,0.67]	15.4 [13.7,17.3]	6.1 [5.3,7.0]
Esophagus (D_{mean})	0.66 [0.61,0.70]	0.75 [0.71,0.80]	23.8 [18.6,29.3]	5.8 [4.0,7.8]
Mandible (D_{mean})	0.88 [0.85,0.90]	0.94 [0.92,0.95]	6.1 [4.7,7.6]	1.6 [1.3,1.9]

Table 2.2: Summary measures (sample mean [bootstrapped 95% confidence interval]) for volumetric and surface metrics of auto-contours of RayStation 10B.

2.6.3 Automated Planning

For automated planning, we replicated the beam setup, OAR/target objectives for both photon and proton as per our institutions clinical head-and-neck protocol.

For photon (Table 2.3), our VMAT plans are made on an isotropic dose grid of 0.2cm The photon beams were commissioned on an Elekta Synergy system with Agility multi-leaf collimator.

For proton (Table 2.4), our IMPT plans are made on an isotropic dose grid of 0.3cm. This dose is delivered using pencil beam scanning (PBS) on a Varian ProBeam machine.

Step	RoI	Function	Description	Weight
1	PTV (DL1)	MinDose	100% of DL1 prescription	80.0 → {*VDT*}
1	PTV (DL1)	MaxDose	102% of DL1 prescription	50.0 → {*VDT*}
1	ring ≤ PTV (DL1)	MaxDose	96% of DL1 prescription	0.0 → {*VDT*}
1	PTV (DL2)	MinDose	100% of DL2 prescription	80.0 → {*VDT*}
1	PTV (DL2)	MaxDose	102% of DL2 prescription	50.0 → {*VDT*}
1	PTV (DL2)	UniformDose	100% of DL2 prescription	10.0
1	Body	DoseFallOff	From 100% to 0% of DL1 prescription over 5.0 cm	1.0
1	Body	DoseFallOff	From 100% to 26% of DL1 prescription over 2.0 cm	2.0
1	Body	DoseFallOff	From 100% to 64% of DL1 prescription over 0.5 cm	10.0
1	Ghost$_{Cranial}$	DoseFallOff	From 100% to 0% of DL1 prescription over 1.0 cm	0.5
1	Ghost$_{Ear(L)}$	DoseFallOff	From 100% to 46% of DL1 prescription over 2.0 cm	1.0
1	Ghost$_{Ear(R)}$	DoseFallOff	From 100% to 46% of DL1 prescription over 2.0 cm	1.0
1	Brainstem	MaxEUD	eudParameterA=50 (maxEUD=4000 cGy)	3.0
1	Brainstem (+3 cm)	MaxEUD	eudParameterA=50 (maxEUD=4400 cGy)	3.0
1	Spinal Cord	MaxEUD	eudParameterA=50 (maxEUD=4000 cGy)	3.0
1	Spinal Cord (+3 cm)	MaxEUD	eudParameterA=50 (maxEUD=4400 cGy)	3.0
2.1	Other Organs	DoseFallOff	From 100% to 20% of DL1 prescription over 2.0 cm	1.0
2.2	Other Organs	DoseFallOff	From 100% to 0% of DL1 prescription over 2.0 cm (*as determined by treatment planner*)	1.0
3	Other Organs	MaxEUD	eudParameterA=50, maxEUD={*VDT*}	1.0
4	Control Structures	{MinDose, MaxDose}	Dose={*VDT*}	{*VDT*}

Table 2.3: Our 4-step emulation of the manual photon optimization process of our clinic. In each step, we also optimize for the objectives of the previous steps. We use *VDT* as an abbreviation for the phrase "value determined by treatment planner". The → indicates that the weight is modified at the end of Step 4.. Here DL1/DL2 stands for electives/boost regions of the tumor and prescription refers to a value of cGy that was assigned to a region-of-interest (RoI). Here "Other Organs" refers to Cochlea (L/R), Parotid (L/R). Submandibular (L/R), Muscle Constrictor (S/M/I), Cricopharyngeus, Larynx (SG), Glottic Area, Trachea, Esophagus and Oral Cavity. The rows shown here are created as objectives in our clinic's treatment planning solution.

Step	RoI	Function	Description	Weight	Robust
1	CTV (DL1)	MinDose	100% of DL1 prescription	$800.0 \rightarrow$ *{VDT}*	*
1	CTV (DL1) - (CTV(DL2) + 3 mm)	MaxDose	102% of DL1 prescription	$20.0 \rightarrow$ *{VDT}*	*
1	CTV (DL1) - (CTV(DL2) + 2 cm)	MaxDose	102% of DL1 prescription	$80.0 \rightarrow$ *{VDT}*	*
1	CTV (DL2)	MinDose	100% of DL2 prescription	$800.0 \rightarrow$ *{VDT}*	*
1	CTV (DL2)	MaxDose	100% of DL2 prescription	$50.0 \rightarrow$ *{VDT}*	*
1	CTV (L)	MinDose	0 cGy and Beam={1,2,3}	0.0	
1	CTV (R)	MinDose	0 cGy and Beam={4,5,6}	0.0	
1	Body	DoseFallOff	From 101% to 0% of DL2 prescription over 2.0 cm	1.0	
1	Body	MaxDose	67% of DL2 prescription for each beam	10000.0	
1	Body	MaxDose	107% of DL2 prescription	100.0	*
2	Mandible	MaxDose	107% of DL2 prescription	$500.0 \rightarrow$ *{VDT}*	*
2	Organ Set 1	DoseFallOff	From 101% to 0% of DL2 prescription over 2.0 cm	1.0	
2	Organ Set 2	DoseFallOff	From 101% to 0% of DL2 prescription over 2.0 cm	1.0	
3.1	Organ Set 2	MaxEUD	eudParameterA=1, maxEUD=*{VDT}*	1.0	
3.2	Organ Set 2 - (CTV (DL1) + 3 mm)	MaxEUD	eudParameterA=1, maxEUD=*{VDT}*	1.0	
4	Control Structure	{MinDose, MaxDose}	Dose=*{VDT}*	*{VDT}*	{*}

Table 2.4: Our 4-step emulation of the manual proton optimization process of our clinic. In each step, we also optimize for the objectives of the previous steps. We use *VDT* as an abbreviation for the phrase "value determined by treatment planner". The $\rightarrow$ indicates that the weight is modified at the end of Step 4.. Here DL1/DL2 stands for elective/boost regions of the CTV and prescription refers to a value in cGy that was assigned to a region-of-interest (RoI). "Organ Set 1" refers to Mandible, Brainstem, Spinal Cord, Esophagus, Trachea, Larynx (SG), Trachea and Glottic Area, while "Organ Set 2" refers to Parotid (L/R), Submandibular (L/R), Muscle Constrictor (S/M/I), and Oral Cavity. The $*$ mark is used to indicate those objectives which are robustly optimized. The rows shown here are created as objectives in our clinic's treatment planning solution.

2.6.4 Organ Dose Metrics

We show dose metrics for organs available in the RayStation 10B auto-contouring module for photon (Table 2.5 and Table 2.6) and proton (Table 2.7 and Table 2.8). For the purpose of our study, we only included organs with available auto-contours, although additional organs-at-risk are evaluated clinically.

RoI	$|P_{OG} - P_{MC}|$	$|P_{MC} - P_{AC}|$
Spinal Cord ($D_{0.03cc}$)	1.45 [0.06,5.51]	1.13 [0.18,5.16]
Brainstem ($D_{0.03cc}$)	1.88 [0.05,6.77]	2.17 [0.21,6.37]
Parotid (L) (D_{mean})	0.12 [0.02,0.72]	0.32 [0.02,2.10]
Parotid (R) (D_{mean})	0.13 [0.01,0.68]	0.42 [0.03,1.66]
Submand (L) (D_{mean})	0.27 [0.02,1.20]	0.45 [0.05,2.37]
Submand (R) (D_{mean})	0.21 [0.01,1.28]	0.35 [0.04,1.80]
Oral Cavity (D_{mean})	3.24 [0.01,0.86]	0.35 [0.05,1.32]
Larynx (SG) (D_{mean})	0.39 [0.03,1.47]	0.39 [0.21,4.24]
Esophagus (D_{mean})	0.24 [0.01,1.64]	0.65 [0.04,3.43]
Mandible ($D_{2\%}$)	0.37 [0.03,3.43]	0.43 [0.06,2.12]

Table 2.5: Median [5th percentile, 95th percentile] of the absolute dose metric values (in Gy) for $P_{OG} - P_{MC}$ and $P_{MC} - P_{AC}$ in photon radiotherapy.

RoI	$|P_{OG} - P_{MC}|$	$|P_{MC} - P_{AC}|$
Spinal Cord ($D_{0.03cc}$)	2.01 [1.51,2.56]	1.90 [1.49,2.32]
Brainstem ($D_{0.03cc}$)	2.43 [1.90,3.01]	2.82 [2.36,3.34]
Parotid (L) (D_{mean})	0.21 [0.15,0.28]	0.66 [0.49,0.85]
Parotid (R) (D_{mean})	0.21 [0.15,0.27]	0.62 [0.48,0.80]
Submand (L) (D_{mean})	0.39 [0.30,0.49]	0.80 [0.52,1.22]
Submand (R) (D_{mean})	0.33 [0.23,0.45]	0.59 [0.42,0.80]
Oral Cavity (D_{mean})	0.32 [0.24,0.42]	0.49 [0.40,0.58]
Larynx (SG) (D_{mean})	0.55 [0.39,0.74]	1.65 [1.25,2.07]
Esophagus (D_{mean})	0.41 [0.29,0.54]	1.05 [0.80,1.38]
Mandible ($D_{2\%}$)	0.81 [0.48,1.22]	0.97 [0.54,1.60]

Table 2.6: Sample mean [bootstrapped 95% confidence interval] of the absolute dose metric values (in Gy) for $P_{OG} - P_{MC}$ and $P_{MC} - P_{AC}$ in photon radiotherapy.

RoI	$|P_{OG} - P_{MC}|$	$|P_{MC} - P_{AC}|$
Spinal Cord ($D_{0.03cc}$)	2.08 [0.03,8.82]	0.70 [0.12,2.40]
Spinal Cord ($D_{0.03cc}$) (vw-max)	1.90 [0.05,8.07]	0.72 [0.15,2.57]
Brainstem ($D_{0.03cc}$)	0.72 [0.05,3.79]	0.59 [0.03,2.77]
Brainstem ($D_{0.03cc}$) (vw-max)	0.98 [0.13,4.30]	1.00 [0.19,2.81]
Parotid (L) (D_{mean})	0.10 [0.02,0.39]	0.48 [0.07,1.99]
Parotid (R) (D_{mean})	0.14 [0.01,0.43]	0.40 [0.03,1.80]
Submand (L) (D_{mean})	0.21 [0.06,0.79]	0.28 [0.05,1.85]
Submand (R) (D_{mean})	0.18 [0.03,0.70]	0.27 [0.01,1.89]
Oral Cavity (D_{mean})	0.08 [0.02,0.39]	0.31 [0.03,0.73]
Larynx (SG) (D_{mean})	0.37 [0.01,1.36]	0.56 [0.19,3.26]
Esophagus (D_{mean})	0.31 [0.01,3.03]	0.23 [0.07,0.77]
Mandible ($D_{2\%}$)	0.44 [0.01,2.19]	0.79 [0.06,2.92]
Mandible ($D_{2\%}$) (vw-max)	0.52 [0.01,2.98]	0.46 [0.08,2.13]

Table 2.7: Median [5th percentile, 95th percentile] of the absolute dose metric values (in Gy) for $P_{OG} - P_{MC}$ and $P_{MC} - P_{AC}$ in proton radiotherapy.

RoI	$|P_{OG} - P_{MC}|$	$|P_{MC} - P_{AC}|$
Spinal Cord ($D_{0.03cc}$)	2.92 [1.93,4.00]	0.92 [0.65,1.20]
Spinal Cord ($D_{0.03cc}$) (vw-max)	2.93 [1.92,4.06]	1.08 [0.79,1.40]
Brainstem ($D_{0.03cc}$)	1.07 [0.67,1.54]	0.89 [0.60,1.20]
Brainstem ($D_{0.03cc}$) (vw-max)	1.35 [0.90,1.84]	1.27 [0.92,1.70]
Parotid (L) (D_{mean})	0.16 [0.11,0.21]	0.63 [0.43,0.87]
Parotid (R) (D_{mean})	0.15 [0.11,0.20]	0.62 [0.41,0.86]
Submand (L) (D_{mean})	0.32 [0.20,0.47]	0.51 [0.32,0.73]
Submand (R) (D_{mean})	0.27 [0.18,0.37]	0.71 [0.29,1.41]
Oral Cavity (D_{mean})	0.15 [0.10,0.21]	0.34 [0.26,0.42]
Larynx (SG) (D_{mean})	0.59 [0.39,0.83]	0.88 [0.54,1.30]
Esophagus (D_{mean})	0.75 [0.42,1.19]	0.34 [0.25,0.45]
Mandible ($D_{2\%}$)	0.88 [0.49,1.40]	1.00 [0.69,1.34]
Mandible ($D_{2\%}$) (vw-max)	0.95 [0.58,1.36]	0.79 [0.54,1.08]

Table 2.8: Sample mean [bootstrapped 95% confidence interval] of the absolute dose metric values (in Gy) for $P_{OG} - P_{MC}$ and $P_{MC} - P_{AC}$ in proton radiotherapy.

2.6.5 NTCP

For NTCP scores (Table 2.9 and Table 2.10), we used the formulae and parameters from the National Indication Protocol for Proton therapy (*Landelijk Indicatie Protocol Protonentherapie*) [103]. From this document, we referred to Section 3.3.3 and 3.3.4 for xerostomia and Section 3.4.3 and 3.4.4 for dysphagia. For all four toxicities, we used a baseline score of 0.

	Photon		Proton	
	$|P_{OG} - P_{MC}|$	$|P_{MC} - P_{AC}|$	$|P_{OG} - P_{MC}|$	$|P_{MC} - P_{AC}|$
Xerostomia Grade ≥ 2	0.1 [0.0,0.5]	0.3 [0.0,0.9]	0.1 [0.0,0.3]	0.2 [0.0,1.0]
Xerostomia Grade ≥ 3	0.0 [0.0,0.2]	0.1 [0.0,0.3]	0.0 [0.0,0.1]	0.1 [0.0,0.3]
Dysphagia Grade ≥ 2	0.2 [0.0,0.9]	0.2 [0.0,0.6]	0.0 [0.0,0.3]	0.1 [0.0,0.3]
Dysphagia Grade ≥ 3	0.1 [0.0,0.7]	0.1 [0.0,0.5]	0.0 [0.0,0.1]	0.0 [0.0,0.1]

Table 2.9: Summary measures (median [5th percentile, 95th percentile]) for ΔNTCP (%) values in photon and proton radiotherapy for $|P_{OG} - P_{MC}|$ and $|P_{MC} - P_{AC}|$.

	Photon		Proton	
	$|P_{OG} - P_{MC}|$	$|P_{MC} - P_{AC}|$	$|P_{OG} - P_{MC}|$	$|P_{MC} - P_{AC}|$
Xerostomia Grade ≥ 2	0.2 [0.1,0.2]	0.4 [0.3,0.4]	0.1 [0.1,0.2]	0.3 [0.2,0.5]
Xerostomia Grade ≥ 3	0.1 [0.0,0.1]	0.1 [0.1,0.2]	0.0 [0.0,0.1]	0.1 [0.1,0.2]
Dysphagia Grade ≥ 2	0.3 [0.2,0.4]	0.2 [0.2,0.3]	0.1 [0.1,0.1]	0.1 [0.1,0.1]
Dysphagia Grade ≥ 3	0.2 [0.1,0.3]	0.2 [0.1,0.2]	0.0 [0.0,0.0]	0.0 [0.0,0.0]

Table 2.10: Sample mean [bootstrapped 95% confidence interval]) for ΔNTCP (%) values in photon and proton radiotherapy for $|P_{OG} - P_{MC}|$ and $|P_{MC} - P_{AC}|$.

2.6.6 Visual Results

(a) Brainstem (DICE=0.83, $|\Delta D_{0.03cc}| = 5.3\%$)

(b) Brainstem (DICE=0.81, $|\Delta D_{0.03cc}| = 28.1\%$)

(c) Submand (R) (DICE=0.90, $|\Delta D_{mean}| = 1.4\%$)

(d) Submand (L) (DICE=0.00, $|\Delta D_{mean}| = 0.5\%$)

(e) Oral Cavity (DICE=0.42, $|\Delta D_{mean}| = 4.1\%$)

(f) Oral Cavity (DICE=0.87, $|\Delta D_{mean}| = 2.4\%$)

(g) Spinal Cord (DICE=0.80, $|\Delta D_{0.03cc}| = 11.2\%$)

(h) Spinal Cord (DICE=0.57, $|\Delta D_{0.03cc}| = 21.8\%$)

(i) Submand (R) (DICE=0.82, $|\Delta D_{mean}| = 1.3\%$)

(j) Submand (R) (DICE=0.80, $|\Delta D_{mean}| = 2.6\%$)
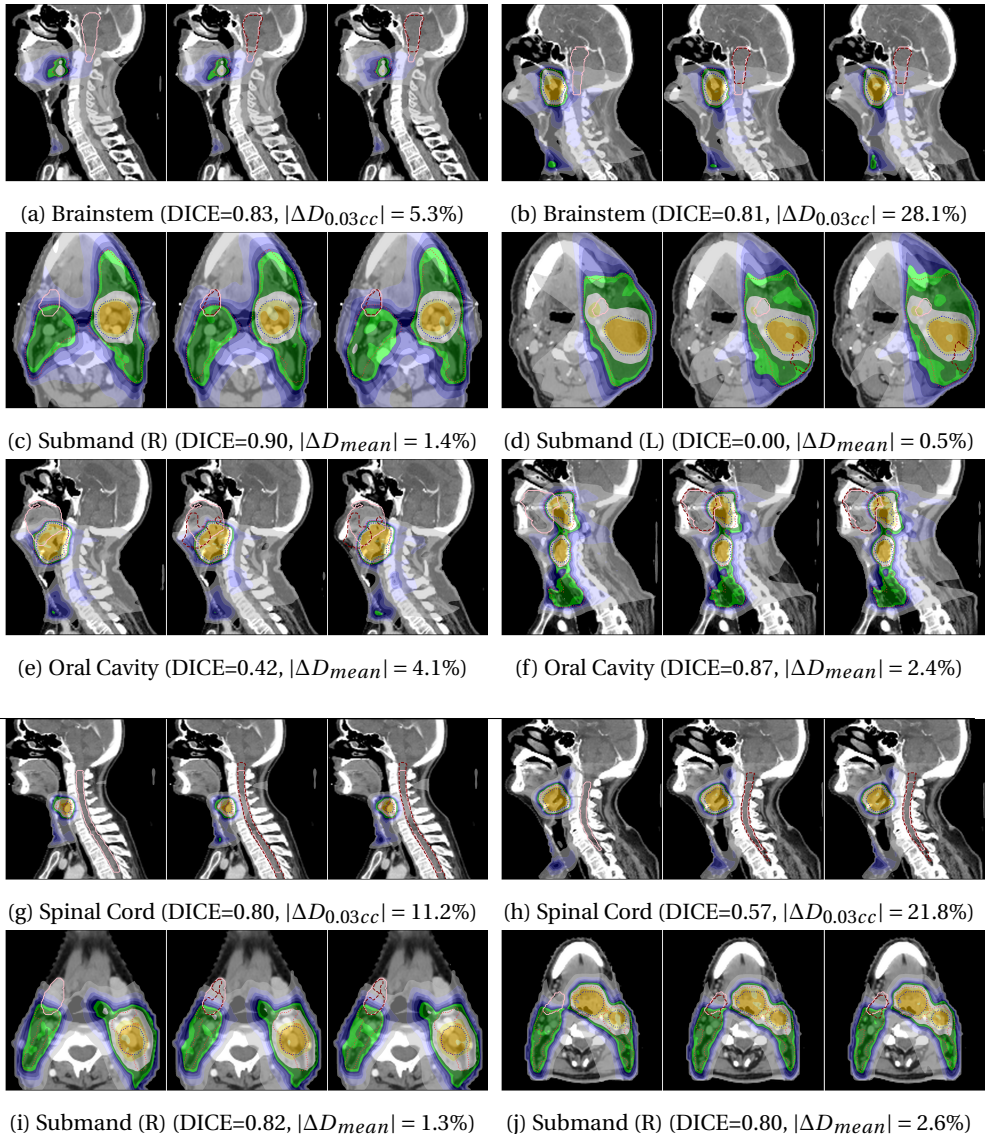
Figure 2.7: This figure shows CT scans of photon (a-f) and proton (g-j) patients overlayed with a dose distribution as well as PTV (DL1) (orange), PTV (DL2) (blue), manual (pink) and automated (maroon) contours. Each example shows the P_{OG}, P_{MC} and P_{AC} plans from left to right. The dose metric in the sub-captions compares the absolute percentage difference of $P_{MC} - P_{AC}$.